Available online at www.sciencedirect.com
SCIENCE DIRECT®

Journal of the European Ceramic Society 24 (2004) 2005–2013

www.elsevier.com/locate/jeurceramsoc

An investigation of co-fired varistor-ferrite materials

Aran Rafferty[a,*], Yurii Gun'ko[a], Ramesh Raghavendra[b]

[a]*Chemistry Department, University of Dublin, Trinity College, College Green, Dublin 2, Ireland*
[b]*Littelfuse (Ireland) Ltd. Ecco Rd., Dundalk, Co. Louth, Ireland*

Received 19 December 2002; received in revised form 6 May 2003; accepted 17 May 2003

Abstract

The purpose of this work was to co-fire crack-free varistor-ferrite ceramic multilayers fabricated via a dry pressing route. Multilayers were sintered using a standard industrial grade varistor sintering regime. Sinter shrinkages of both varistor and ferrite materials were measured using dilatometry and showed that the varistor shrunk significantly more than the ferrite material. X-ray diffraction analysis indicated that no significant phase changes occurred in the materials under investigation as a result of the sintering process. Scanning electron microscopy observations of the dry-pressed co-fired varistor-ferrite revealed vertical cracking in the ferrite due to thermal expansion mismatch between the materials. By pressing a mixed composition interlayer in the ratio 50:50, between the varistor and ferrite materials, a crack-free multilayer structure could be obtained. Energy dispersive X-ray analysis of the co-fired ferrite and varistor confirmed diffusion of Fe and Ni components from the ferrite into the varistor material. The degree of diffusion was reduced by using 50:50 ratio mixed composition interlayers.

Keywords: Diffusion; Ferrites; Pressing; Varistors; ZnO

1. Introduction

ZnO varistors are semiconducting ceramics having highly non-ohmic current-voltage characteristics which are fabricated by sintering of ZnO powders with small amounts of additives such as Bi_2O_3, CoO, MnO and Sb_2O_3.[1] The non-ohmic property comes from grain boundaries between the semiconducting ZnO grains. Due to their superior electrical properties, these materials have become important as varistor materials for voltage surge protectors in electrical circuits.[2] Varistors provide bidirectional transient protection and are very effective in suppressing high amplitude and low-frequency transients.

However, modern day electronic components, mainly based on silicon are more susceptible, not only to electrical overvoltage transients, but also to damage by electronmagnetic pulses or electromagnetic interference (EMI) noise that is now strictly regulated by law throughout the world. EMI is a degradation in performance of an electronic system caused by an electromagnetic disturbance. The means of noise transmission are conduction and radiation. The effective counter to radiation is shielding; radiated energy is absorbed by the shielding and dissipated as heat. The effective measure against conduction is the EMI filter, which diverts conducted energy away from the protected system to ground. EMI filters are fabricated from a combination of capacitors and inductors utilising their different impedance characteristics to reduce unwanted signals, selectively. Simple, single component filters are known as capacitor or inductor filters, while a combination of a single inductor and a single capacitor is known as an "L" filter. A combination of a pair of inductors and a single capacitor is known as a "T" filter and a combination of a single inductor with a pair of capacitors is known as a "Pi" filter.

For this reason, ferrite components can be used as the inductor component and varistor as the capacitor component, to equip the electronics industry with high performance, cost-effective filters to control troublesome EMI. Ni–Zn ferrites are soft ferrimagnetic ceramic materials and are commonly the ferrites of choice for EMI applications, having very high resistivity, high

* Corresponding author.
E-mail addresses: rafferta@tcd.ie (A. Rafferty), igounko@tcd.ie (Y. Gun'ko), rraghavendra@littelfuse.com (R. Raghavendra).

0955-2219/03/$ - see front matter © 2003 Elsevier Ltd. All rights reserved.
doi:10.1016/S0955-2219(03)00361-3

permeability values and little eddy current loss in high frequency operations.[3] Ferrite components are known to be efficient and cost-effective for the prevention of spurious signals transmitted by conductance and by radiation. Yue et al.[4] investigated the properties of ferrite–cordierite composites for use in multilayer chip inductors and point out that substrates with high permeability may decrease EMI between components in integrated circuits. Many authors are currently experimenting with different methods of depositing ferrite films. Sedlar et al.[5] report on a dip coating sol-gel approach to be used in the development of fibre-optic magnetic field sensors. Welch et al.[6] and Keller et al.[7] prepared NiZn and $NiO/\alpha Fe_2O_3$ multilayer films by pulsed laser deposition while other authors[8,9] have used a reactive vapor deposition process and a ferrite plating process respectively.

The multilayers under investigation here were fabricated by dry pressing. Dry pressing may be defined as the simultaneous uniaxial compaction and shaping of a granular powder with small amounts of water and/or organic binders during confined compression in a die. The extensive practice of dry pressing stems from the inherent ability to form rapidly a wide variety of shapes with close tolerances and controlled compact character using highly mechanized and automated equipment. Steatites, aluminas, titanates and ferrites have been dry pressed in sizes ranging from a few mm to several inches in linear dimensions at rates of up to 5000 parts per minute on smaller parts.[10] However, as a result of the minaturisation of electronic circuits and increased component densities in circuit boards, it became logical to develop multi-layer devices in favour of earlier monolayer dry pressed devices, because of their compact size, good temperature and voltage characteristics and low manufacturing cost.[11] In varistor technology, by using an intercalated electrode–ZnO inter-layer design the available cross-sectional functional area is greatly increased, with the consequence of diverting transient over-voltages more effectively.[12] Furthermore the compact arrangement improves the energy and power dissipation capabilities of the device. The emergence of multilayer devices meant that an alternative to dry powder pressing had to be devised, whereby manifold ceramic layers could be deposited and built up quickly and efficiently. Two basic processes to have gained acceptance for the manufacture of multi-layer components are screen-printing and tape-casting. In screen-printing the ceramic powders are mixed with suitable organic binders to prepare ceramic inks. The inks are laid down, dried and built up sequentially. Multilayer devices developed to date include multilayer ceramic capacitors, multilayer piezoelectric ceramic actuators, multilayer chip inductors and their integration into a low-temperature cofired ceramic substrate called a high density package.[13] Multilayer piezoelectric ceramics have been widely used as micro-displacement actuators.[14] Compared with ceramic pellet and bimorph structures, multilayer piezoelectric actuators have several advantages, such as small drive voltage, quick response, large generative force, and high electromechanical coupling.

Cai et al.,[11] report on the successful development of low-sintering composite multilayer ceramic capacitors (CMLCC's) via tape casting and screen printing techniques. They used four kinds of Pb based dielectrics separated by inner Ni electrodes. They highlight matching of materials properties, and in particular shrinkage rate, which is the derivative of the densification curve with respect to time, as being critical in the material design of CMLCCs. Zuo et al.,[13] investigated the interfacial interaction between cofired Pb-based complex relaxor ferro-electrics and Ag/Pd electrodes. Undesired interfacial defects, including delaminations, warping, pores, and exaggerated grain growth were observed. Zuo et al. blame these microstructural defects on mismatched physical and chemical properties, the unsuitable preparation process and different electrode compositions. In a related study Zuo et al.[15] conducted EDX experiments which demonstrated vapour diffusion of silver to a depth of several microns through the Pb-based ceramic. Not only therefore are there problems associated with thermal mismatch, shrinkage mismatch, poor interfaces, delamination and cracking, but also material diffusion or contamination which is a key concern and can have a deleterious effect on electrical properties. Where the semiconductive ceramic composition comprises ZnO and the magnetic ceramic composition comprises a Ni–Zn ferrite, Ni and Fe compounds may diffuse into the varistor material. The diffusion of Ni and Fe compounds can result in deterioration of both the varistor characteristics and the capacitor characteristics of the semiconductive ceramic composition. As a result of the diffusion, the linearity for the varistor characteristics may be lowered and the dielectric loss for the capacitor characteristics increased.

Co-firing of ceramics, whether by a dry pressing or screen printing technique is widely regarded as a difficult and precarious task. Sarraute et al.[16] investigated a dry-pressing fabrication process to produce $BaTiO_3$–Ni–Zn ferrite functionally graded multilayer ceramics. They obtained a crack free non-symmetric configuration multilayer by sequentially stacking, pressing and sintering. They identify thermal expansion mismatch between the materials as being the primary difficulty, but overcame this by using mixed composition ceramic mixes as multilayers between the barium titanate and ferrite materials. Meanwhile, in a closely related paper, Sorensen et al.[17] use a fracture mechanics approach to investigate steady-state delamination of multilayered structures caused by stresses arising during processing due to thermal expansion mismatch. According to

Sorensen et al., delamination arises because the interface between two material compositions often possesses a lower fracture toughness than the bulk materials. Secondly, residual stresses may develop in the layers during processing due to differences in the thermal expansion coefficients, phase transitions, grain growth, point defect annihilation, etc. Furthermore, a complicated stress state exists at free edges of a layered material, if the elastic properties differ from layer to layer and it is thus likely that delamination can start from the edges. They found that inserting just a few interlayers with intermediate thermal expansion coefficients is an effective way of reducing the delamination energy release rate. He et al.,[18] report on bilayered lead zirconate titanate (PZT) based ceramics successfully fabricated by a simple dry-pressing and free sintering process. One layer was designed for high remanent polarization, because this is the base for ferroelectric material showing good performance. The other layer was expected to possess low dielectric loss, because this is related to long lifetime. He et al. proved that the method employed was a feasible method of making a good performance and long service time prototype composite component, exhibiting combined properties of high remanent polarazition and low dielectric loss.

Dry pressing technology therefore, although limited, does allow for the making of test prototype layered structures, which if successful should allow for commercial development of multilayer devices via a ceramic ink screen-printing process.[19] Much research has focused on integrated passive devices, or devices having more than one function within a single device. One obvious area of interest is the creation of a composite functional device by integrally sintering varistor and ferrite materials. Here we report on the preparation of multi-layered varistor–NiZn ferrite structures and investigate sinter shrinkage, microstructure and cross-boundary diffusion.

2. Experimental procedure

2.1. Powder preparation

The materials used in this study were a ZnO industrial grade varistor powder (Littelfuse Ltd. Dundalk, Ireland) with a sintering temperature of 1130 °C and two industrial grades of magnetic Ni–Zn ferrite powder (MMG Neosid Ltd., UK). The ferrite powders will be referred to as Ferrite A, which has a sintering temperature of 1170° and Ferrite B, which has a sintering temperature of 1280 °C. The elemental compositions as determined by EDX analysis are detailed in Table 1.

The varistor composition is made by weighing and mixing of the appropriate reagents. The mixes are ball-milled for 6 h to achieve a homogenous mixture. The mixed components are then calcined at a temperature of 800 °C for 6 h to reduce the carbonates, thus reducing the evolution of gases during the final sintering stage.

Table 1
Elemental compositions of varistor and ferrite powders

Element/At%	Varistor	Ferrite A	Ferrite B
Zn	94.03	15.36	20.34
Fe	–	67.29	68.21
Ni	–	14.5	9.56
V	–	2.45	–
Sb	3.35	–	–
Mn	0.61	0.39	1.89
Co	0.63	–	–
Bi	0.68	–	–
Cr	0.70	–	–

Mixtures of varistor/ferrite A and varistor/ferrite B were made up in 50:50 weight% ratios to be used as interlayers. These were ground together in a mortar and pestle and ball milled for 4 h to ensure a homogeneous mixture. These will hereafter be referred to as interlayer A and interlayer B respectively.

2.2. Powder pressing

Prior to pressing, the chosen powders were ground in a mortar and pestle and then ball milled for 4 h. Pellets were pressed using a manual 15 t hydraulic press (Specac Ltd. Kent, UK). and a 7 mm evacuable pellet die (Specac Ltd. Kent, UK). For multilayer pellets comprising ferrite, multilayer and varistor, an optimum pressing procedure was developed. In this way the first powder is added to the die and pressed for 20 s under 1 t pressure to form a pellet. Then the second powder is added to the die and pressed against the previously formed pellet for 20 s, leading to a co-pressed bi-layer sample. Finally the third powder is added to the die and pressed with the previously co-pressed sample for 60 s, resulting in a triple layered device. Pellets were sintered using a sintering regime normally used for varistor sintering. Samples were ramped from room temperature to 400 °C in 6 h, held at 400 °C for 1 h and then ramped to 1130 °C in 4 h. They were held at 1130 °C for 4 h then ramped down to room temperature in 8 h.

2.3. Dilatometry

A differential thermal dilatometer was used to measure the sintering shrinkage properties of the ceramics. The dilatometer used was a Dil 402 PC (Netzsch) horizontal pushrod type dilatometer with a temperature range of 25 to 1400 °C. Pellets measuring 7 mm in diameter were pressed using a pressure of 1 t for 20 s. These were then sintered using a constant heating rate of 3 °C/min^{-1}, held at 1130 °C for 2 h and cooled in air to room temperature. Die lubrication was carried out at

regular intervals by cleaning with 0.5 wt.% stearic acid dissolved in iso-propanol.

2.4. Scanning electron microscopy (SEM)

Sintered samples were cut perpendicular to the interface, mounted in bakelite and then polished to a 1 μm finish to allow for the observation of the microstructure at the interface and to analyse the compositional profile by energy dispersive X-ray spectroscopy (EDX), (Princeton Gamma-Tech, NJ, USA). The SEM equipment used was an S-3500N variable pressure scanning electron microscope (Hitachi, Japan) with a resolution of 3.5 nm at 25 kV. All samples were ground for 2 min using 1200 grit SiC paper, polished for 5 min with 9 μm diamond polish and finally for a further 5 min using 1 μm diamond polish.

2.5. X-ray diffraction (XRD) analysis

X-ray diffraction (XRD) analysis was carried out on both "green" (before sintering) and sintered samples of Ferrite A, Ferrite B, varistor and mixed interlayer compositions. A Kristallofle X-ray powder diffractometer (Siemens, Germany) was employed using CuK_α X-rays.

3. Results and discussion

Cofiring of ceramic materials is a difficult task and a successful outcome depends on the ability to harness a number of important variables. Differences in thermal coefficients, shrinkage and elastic modulus can lead to stresses (tensile or compressive) and ultimately lead to delamination, micro-cracking or pore formation in the ceramic materials. Phase changes as a result of sintering (e.g. tetragonal to cubic in $BaTiO_3$) can also contribute to sintering mismatch. XRD analysis confirmed that no significant phase changes occurred during sintering of the materials under investigation here. Fig. 1 shows the XRD patterns for Ferrite B, illustrating the presence of identical nickel–zinc–iron phases before and after sintering. Similar patterns were observed for the varistor composition and mixed interlayer compositions.

Dilatometry is widely recognised as an indispensable tool for investigating the sintering shrinkage characteristics of ceramics to be cofired. Fig. 2 shows the sintering shrinkage behaviour of Ferrite A, interlayer A and varistor.

From Fig. 2 it can be seen that there are dramatic differences in the sintering shrinkage behaviour of the varistor and ferrite A materials. Ferrite A begins to densify at a lower temperature, sinters gradually and finishes up with a linear shrinkage of approximately 13%. The varistor begins to shrink after the ferrite and then the gradient is very sharp with a final linear shrinkage of approximately 18%. There is thus quite a large degree of mismatch between the materials in terms of shrinkage. This is believed to be due to the lack of liquid phase for the ferrite material, as opposed to the varistor material, which contains additives such as Bi_2O_3 and Sb_2O_3. Lu et al.[20] report rapid shrinkage of zinc oxide-based varistors containing additions of Bi_2O_3 and Sb_2O_3 at around 1000 °C. They attribute this rapid shrinkage to the reaction between the pyrochlore phase and ZnO which accelerates the sintering rate of ZnO through a liquid-phase sintering mechanism. Similarly in ferrites, many authors[21–23] have used sintering additives to induce liquid-phase sintering, thus reducing the sintering temperature. Not only can these additives aid sintering, they can also effect an improvement in properties, such as magnetic permeability.[24] No additions were made to the ferrites under investigation here. As the varistor has higher shrinkage than the ferrite it is

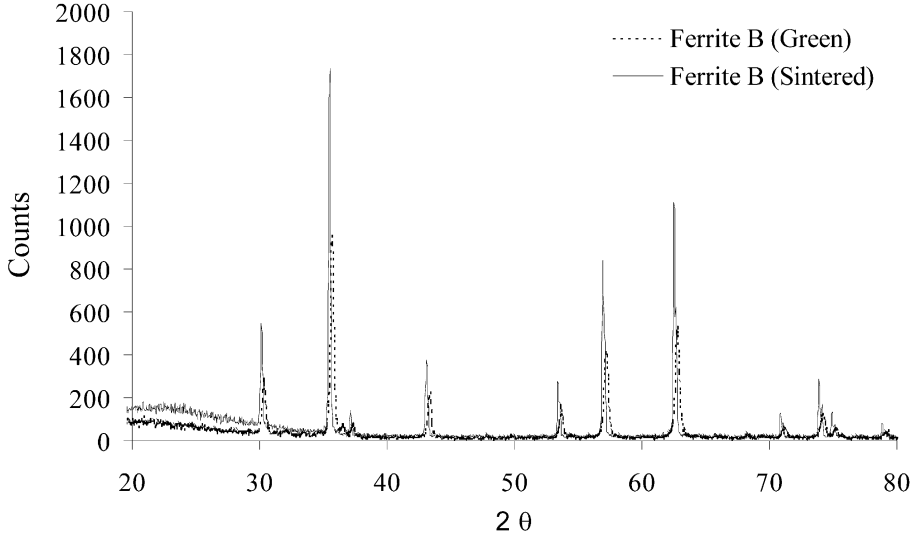

Fig. 1. Overlapping XRD traces of Ferrite B. (-Green-Sintered).

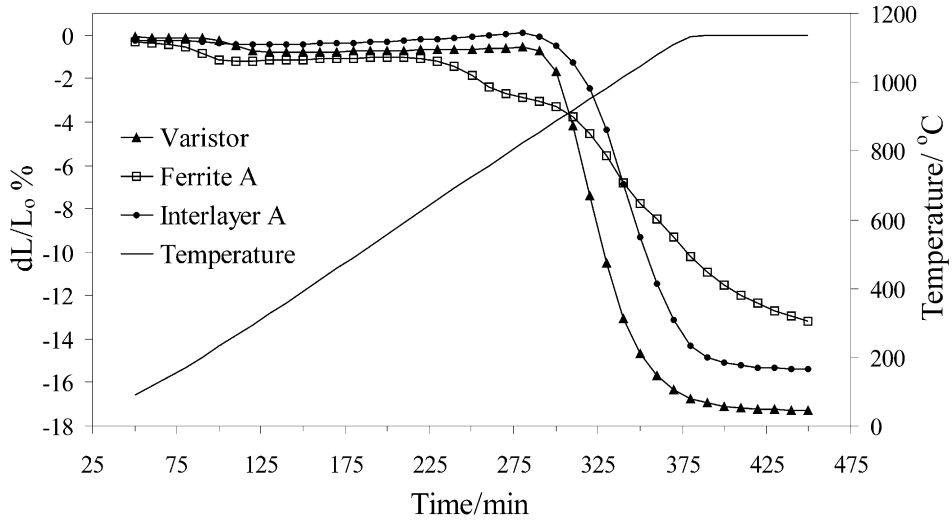

Fig. 2. Dilatometric shrinkage curves of Ferrite A, interlayer A and varistor.

expected that the ferrite is in a state of compression during sintering, a phenomenon that can lead to delamination and cracking.

Bi-layer pellets of varistor and ferrite A were pressed, sintered and analysed using SEM, to see if the shrinkage mismatch was being reflected microstructurally. Fig. 3 is a cross-section of the co-pressed, sintered pellet.

In this study, no cracks were observed in the "green" samples. From Fig. 3, however after sintering cracks are clearly visible in the ferrite material, running perpendicular to the interface. Sarraute et al.,[16] in their study of co-pressed $BaTiO_3$–ferrite pellets observed cracks in their samples. In their case, cracks parallel to the interface were observed at the green stage, induced by the pressing process. Further cracks were observed after sintering, due to thermal mismatch between the layers and these cracks always ran perpendicular to the interface. The cracks in Fig. 3 are clearly due to thermal mismatch between the two materials as reflected in the shrinkage curves in Fig. 1. Of interest in Fig. 2 is the shrinkage characteristic of interlayer A which being a 50:50 ratio mix of varistor and ferrite A is expected to have an intermediate thermal expansion coefficient. From Fig. 2 it is clear that the curve of interlayer A mimics that of the varistor but the shrinkage profile occurs at higher temperatures with the final shrinkage intermediate between varistor and ferrite A. Multilayer pellets of varistor, multilayer A and ferrite A were pressed, sintered and analysed using SEM, to see if the problem of cracking could be eradicated. Fig. 4 is a cross-section of a co-pressed pellet.

From Fig. 4 it can be seen that by using an intermediate 50:50 interlayer a crack-free multilayer device can be fabricated. Sarraute et al.,[16] reported similar success with their $BaTiO_3$–ferrite structures. In the case of Fig. 4 above, the interfaces between the layers are also of good quality, with no evidence of delamination.

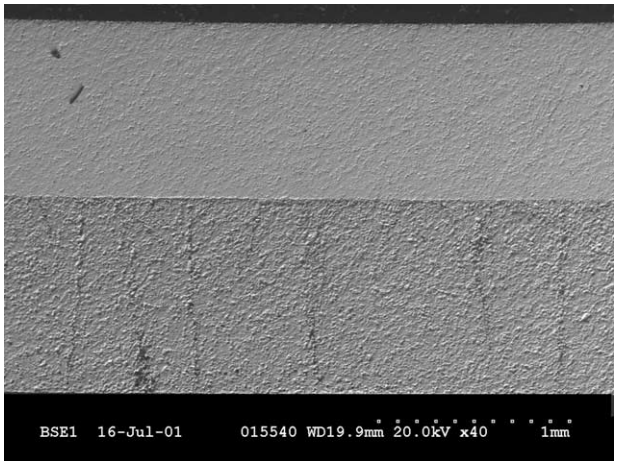

Fig. 3. SEM cross-section of varistor/Ferrite A interface, showing vertical cracks in the ferrite (bottom layer).

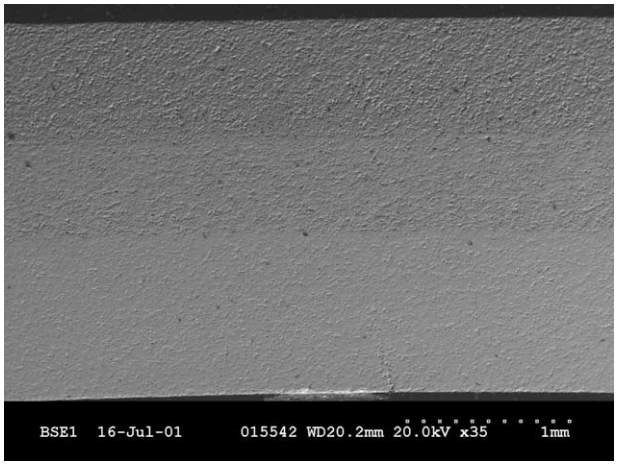

Fig. 4. SEM cross-section of varistor (bottom)/interlayer A/Ferrite A interface showing a crack-free device.

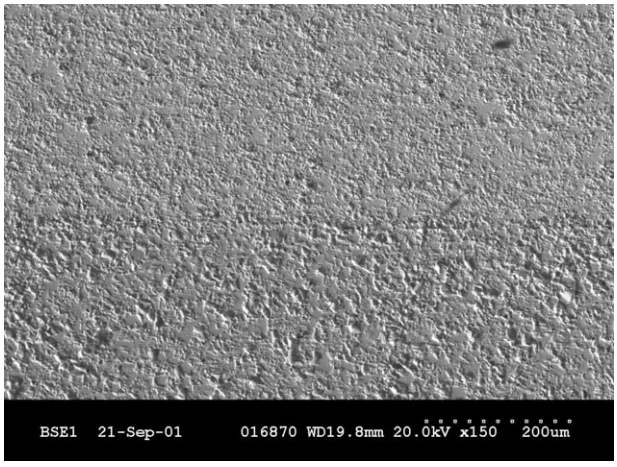

Fig. 5. SEM cross-section of Ferrite A (bottom)/Interlayer A (top) interface.

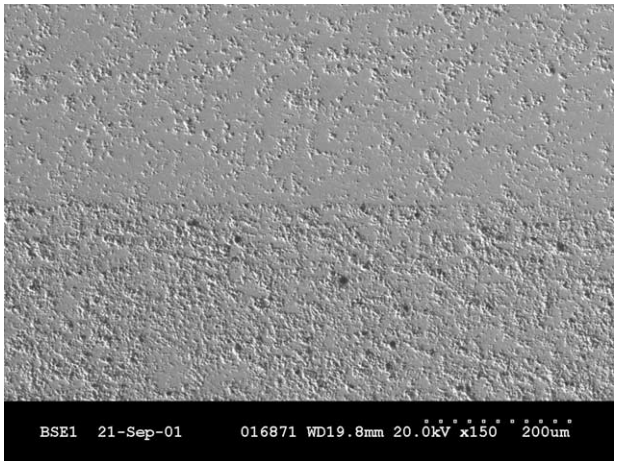

Fig. 6. SEM cross-section of Interlayer A (bottom)/Varistor (top) interface.

Fig. 5 shows the Ferrite A/Interlayer A interface while Fig. 6 shows the Interlayer A/Varistor interface.

Ferrite B was characterised in a similar manner to Ferrite A. Due to the recommended sintering temperature in excess of 1280 °C for ferrite B it was highly speculative as to whether it would be a match with the varistor in terms of sintering and shrinkage. Fig. 7 shows the sintering shrinkage behaviour of Ferrite B, interlayer B and varistor.

From Fig. 7 it is clear that the final shrinkage of Ferrite B is considerably less than the varistor material and also the interlayer material. Furthermore, the densification onset lags behind that of both the varistor material and interlayer material. Again the interlayer curve almost mimics the varistor curve. It is worth noting that on a visual inspection, the cofired pellets were well bonded with flush interfaces. However a gradient could be seen, where the varistor material had noticeably shrunk more than the ferrite and interlayer materials. This was confirmed by SEM analysis where it was found that the shrinkage mismatch manifested itself in a warping effect, although the layers were crack-free with excellent interfaces. See Fig. 8.

From Fig. 8 the effect of the shrinkage mismatch can be seen and it appears that the mechanism of stress release results in a warping of the triple-layer in a concave manner around the varistor material. Sorensen et al.,[17] experienced a similar phenomenon. In response to this Sorensen et al. fabricated some multilayers consisting of five layers, with the two new intermediate layers consisting of mixed powders in the ratio 20/80 and 80/20, respectively. The result of this was crack-free five layer structures with no warping. However, when this approach was adopted by this author it proved unsuccessful, largely due to the difficulty of sequentially pressing five layers in such a small die. While in theory

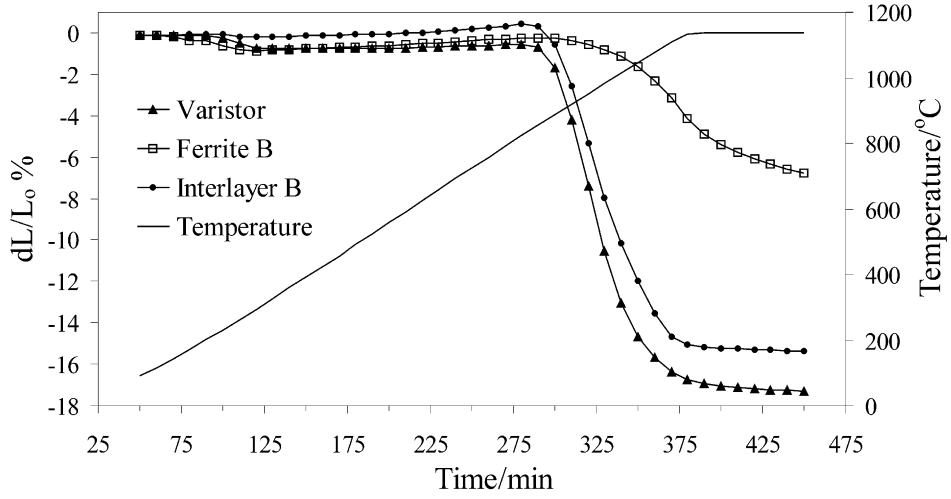

Fig. 7. Dilatometric shrinkage curves of Ferrite B, interlayer B and varistor.

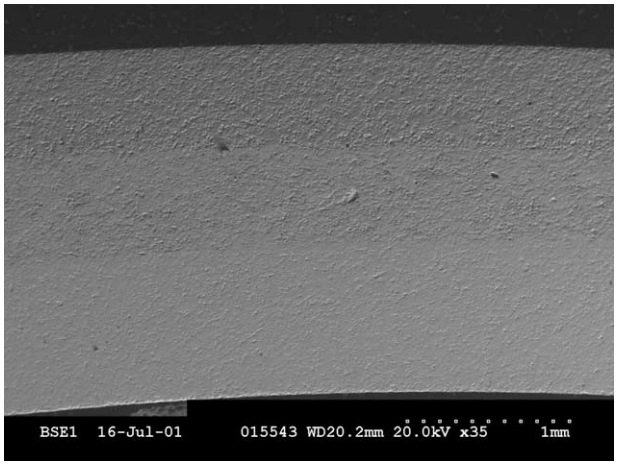

Fig. 8. SEM cross-section of varistor (bottom)/interlayer B/Ferrite B interface, showing a crack-free device.

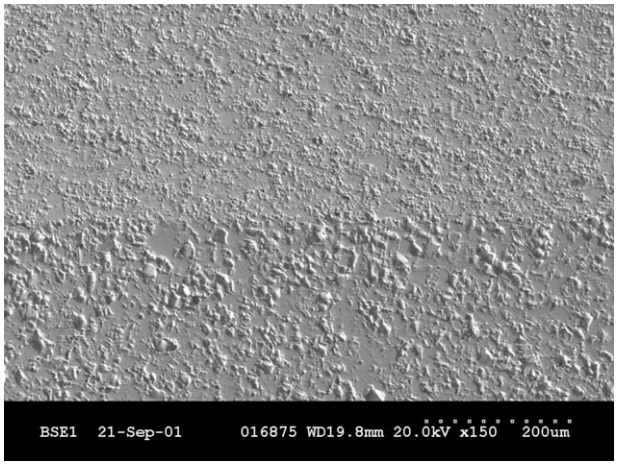

Fig. 9. SEM cross-section of Ferrite B (bottom)/Interlayer B (top) interface.

the five-layer approach is feasible from the point of view of fracture mechanics, in a production sense it is impractical as it introduces too many steps into the process.

The most promising feature of Fig. 8 is the excellent interface quality between the layers. Fig. 9 shows the interface between Ferrite B and Interlayer B while Fig. 10 shows the interface between Interlayer B and varistor.

Fig. 9 and 10 illustrate the excellent interfaces and also a microstructure that is uniform and dense. Furthermore, there is no noticeable interaction layer between the sintered layers. Malic et al.,[25] investigated co-firing of lead–magnesium niobate capacitor and ZnO-based varistor ceramics in the temperature range of 900–1000 °C. "Sandwich" structures obtained by dry pressing revealed a good contact between the parts with no noticeable interaction layer. Selected functional

Table 2
Elemental composition of varistor material in bi-layer and triple layer sintered devices

Sample	100 μm into varistor from interface	200 μm into varistor from interface	300 μm into varistor from interface
(1) Varistor–Ferrite A	51.36 at.% O	51.30 at.% O	50.85 at.% O
	42.77 at% Zn	45.02 at% Zn	45.88 at% Zn
	2.38 at% Fe	1.38 at% Sb	1.07 at% Fe
	1.17 at% Ni	1.13 at% Fe	1.02 at% Sb
	1.67 at% Sb	0.40 at% Ni	0.43 at% Ni
	0.47 at% Cr	0.39 at% Mn	0.37 at% Cr
	0.17 at% Mn	0.37 at% Cr	0.37 at% Mn
(2) Varistor–Ferrite B	50.96 at% O	51.17 at% O	50.97 at% O
	42.20 at% Zn	43.38 at% Zn	43.23 at% Zn
	3.59 at% Fe	1.59 at% Fe	1.54 at% Fe
	1.79 at% Ni	1.38 at% Ni	1.34 at% Ni
	1.25 at% Sb	1.28 at% Sb	1.32 at% Sb
	0.11 at% Cr	0.21 at% Cr	0.32 at% Cr
	0.09 at% Mn	0.18 at% Mn	0.22 at% Mn
(3) Varistor–50:50—Ferrite A	51.04 at% O	50.96 at% O	51.19 at% O
	44.49 at% Zn	45.60 at% Zn	45.48 at% Zn
	1.78 at% Fe	1.15 at% Sb	1.45 at% Sb
	1.25 at% Sb	1.01 at% Fe	0.72 at% Fe
	0.87 at% Ni	0.51 at% Ni	0.34 at% Cr
	0.36 at% Cr	0.36 at% Cr	0.40 at% Ni
	0.21 at% Mn	0.43 at% Mn	0.42 at% Mn
(4) Varistor–50:50—Ferrite B	51.12 at% O	51.10 at% O	51.22 at% O
	44.50 at% Zn	45.22 at% Zn	45.14 at% Zn
	1.35 at% Sb	1.35 at% Sb	1.49 at% Sb
	1.78 at% Fe	1.16 at% Fe	0.84 at% Fe
	0.59 at% Ni	0.39 at% Ni	0.39 at% Ni
	0.30 at% Mn	0.39 at% Mn	0.40 at% Cr
	0.38 at% Cr	0.38 at% Cr	0.50 at% Mn

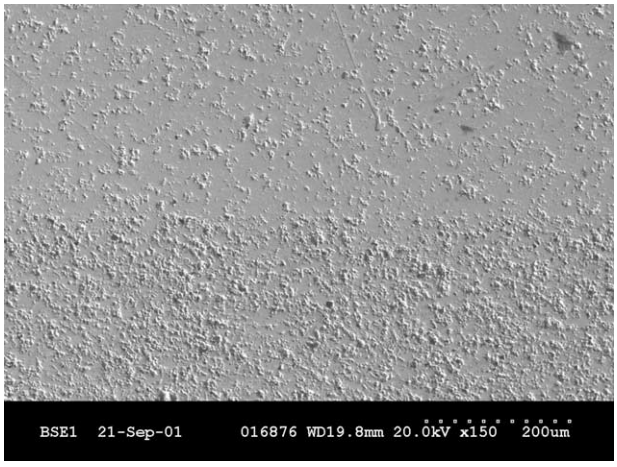

Fig. 10. SEM cross-section of Interlayer B (bottom)/Varistor (top) interface.

properties of the varistor and relaxor parts were reported as adequate. As mentioned earlier, cross-boundary diffusion is a critical feature of the co-firing process and can lead to deleterious functional properties. In order to qualitatively analyse the elemental compositions of the layers under investigation here, energy dispersive X-ray microanalysis (EDX) was employed. Table 2 outlines the results recorded.

From Table 2 we can see that sample (1) contains 2.38 at.% Fe and 1.17 at.% Ni at a depth of 100 μm in from the interface with the ferrite. For sample (3) containing the mixed composition interlayer the iron content reduces to 1.78 at.% Fe and 0.87 at.% Ni at a depth of 100 μm in from the interface with the ferrite. Sample (4) has 3.59 at.% Fe and 1.79 at.% Ni at a depth of 100 μm in from the interface with the ferrite, while the use of the mixed interlayer causes a reduction to 1.78 at.% Fe and 0.59 at.% Ni at a depth of 100 μm in from the interface with the ferrite. Sarraute et al.[16] report a similar occurrence for their $BaTiO_3$–ferrite multilayers. For samples with interlayers they detected the presence of iron close to the interface with the mixed composition layer. One solution to the problem of cross-boundary diffusion may be to use a high-diffusion coefficient barrier layer, with intermediate thermal coefficient.

4. Conclusions

This work shows that it is possible to co-fire crack-free varistor-ferrite multilayers made using dry powder pressing. All the multilayer devices were crack-free in the ''green'' stage prior to sintering. Sintered devices could only be made in an unimpaired condition by using a mixed composition multilayer of intermediate thermal expansion coefficient between the layers of varistor and ferrite. Dilatometric analysis confirmed that this interlayer had a sinter shrinkage intermediate between those of the varistor and ferrite materials. SEM analysis revealed dense, uniform morphologies with excellent interface quality. There was no evidence of cracking or delamination in samples that utilised interlayers. XRD analysis of the ferrites confirmed that no deleterious phase changes were occurring on sintering. EDX analysis showed that diffusion of Fe and Ni components into the varistor was taking place but this was reduced when a multilayer was used between the varistor and ferrite materials.

Acknowledgements

The authors gratefully acknowledge the financial support received from Enterprise Ireland under the aegis of the INNOVATION PARTNERSHIP programme. The authors would also like to thank Sheena Kelly and Kevin Travers for their technical assistance.

References

1. Eda, K., Zinc Oxide Varistors. *IEEE. Elec. Ins. Mag*., 1989, **5**(6), 28–41.
2. Olsson, E., Falk, L. K. L. and Dunlop, G. L., The microstructure of a ZnO varistor material. *J. Mat. Sci*., 1985, **20**, 4091–4098.
3. Costa, A. C. F. M., Tortella, E., Morelli, M. R. and Kiminami, R. H. G. A., Synthesis, microstructure and magnetic properties of Ni–Zn ferrites. *J. Magn. Magn. Mater*., 2002, **256**(1–3), 174–182.
4. Yue, Z., Li, L., Zhang, H., Ma, Z. and Gui, Z., Preparation and electromagnetic properties of ferrite-cordierite composites. *Mater. Lett*., 2000, **44**, 279–283.
5. Sedlar, M., Matejec, V., Grygar, T. and Kadlecova, J., Sol-gel processing and magnetic properties of nickel zinc ferrite thick films. *Ceram. Int*., 2000, **26**, 507–512.
6. Welch, R. G., Neamtu, J., Rogalski, M. S. and Palmer, S. B., Pulsed laser deposition of polycrystalline NiZn ferrite films. *Solid State Comms*., 1996, **97**, 355–359.
7. Keller, N., Guyot, M., Das, A., Porte, M. and Krishnan, R., Study of the interdiffusion at the interfaces of $NiO/\alpha Fe_2O_3$ multilayers prepared by pulsed laser deposition. *Solid State Comms*., 1998, **105**, 333–337.
8. Sohma, M., Kawaguchi, K., Oosawa, Y., Manago, T. and Miyajima, H., Magnetic properties of epitaxial spinel bilayers and multilayers. *J. Magn. Magn. Mater*., 1999, **198-199**, 294–296.
9. Abe, M., Ferrite plating: a chemical method preparing oxide magnetic films at 24–100bk7C, and its applications. *Electro. Acta*, 2000, **45**, 3337–3343.
10. Wang, F. F. Y., *Treatise on Materials Science and Technology; Ceramic Fabrication Processes*. Academic Press, New York, 1976.
11. Cai, H., Gui, Z. and Li, L., Low-sintering composite multilayer ceramic capacitors with X7R specification. *Mats. Sci. Eng. B*, 2001, **83**, 152–157.
12. Puyane, R., Applications and product development in varistor technology. *J. Mats. Pro. Tech*., 1995, **55**, 268–277.
13. Zuo, R., Li, L., Gui, Z., Ji, C. and Hu, X., Vapor diffusion of silver in cofired silver/palladium–ferroelectric ceramic multiplayer. *Mats. Sci. and Eng. B*, 2001, **83**, 152–157.
14. Yao, K. and Zhu, W., Improved preparation procedure and properties for a multilayer piezoelectric think-film actuator. *Sensors and Actuators A*, 1998, **71**, 139–143.

15. Zuo, R., Li, L. and Gui, Z., Interfacial development and microstructural imperfection of multilayer ceramic chips with Ag/Pd electrodes. *Ceram. Int*., 2001, **27**, 889–893.
16. Sarraute, S., Sorensen, T. and Rubaek Hansen, E., Fabrication Process for Barium Titanate-Ferrite Functionally Graded Ceramics. *J. Eur. Ceram. Soc*., 1998, **18**, 759–764.
17. Sorensen, B. F., Sarraute, S., Jorgensen, O. and Horsewell, A., Thermally induced delamination of multilayers. *Acta Metall. Mater*., 1998, **46**, 2603–2615.
18. He, Z., Zhang, J. M. and Li, T., Fabrication and characterisation of bilayered Pb (Zr, Ti)O_3-based ceramics. *Mater. Lett*., 2002, **56**, 1084–1088.
19. Raghavendra, R., Bellew, P. and McLoughlin, N., Copressing of electroceramics technology: a simple IPD for combined transient and EMI suppression applications. *Passive Component Industry, Jan/Feb*, 2002, 13–34.
20. Lu, C., Chyi, N., Wong, H. and Hwang, W., Effects of additives and secondary phases on the sintering behaviour of zinc oxide-based varistors. *Mats. Chem. Phys*., 2000, **62**, 164–168.
21. Wang, S., Wang, Y., Yang, T., Wang, P. and Lu, C., Densification and properties of fluxed sintered NiCuZn ferrites. *J. Magn. Magn. Mater*., 2000, **217**, 35–43.
22. Hozer, L., *Semiconductor Ceramics*. Ellis Horood, England, 1994.
23. Chen, L., His, C., Fu, S. and Lin, J., Cosintering of Ni–Zn–Cu ferrite with low-temperature cofired ceramic substrates. *Jap. J. Appl. Phys*., 2000, **39**, 150–154.
24. Drofenik, M., Znidarsic, A. and Makovec, D., Influence of the addition of Bi_2O_3 on the grain growth and magnetic permeability of MnZn ferrites. *J. Am. Ceram. Soc*., 1998, **81**, 2841–2848.
25. Malic, B., Kosec, M., Razinger, J. and Zivic, Z., Processing and characterisation of cofired capacitor and varistor ceramics. *Mats. Res. Soc. Symp*., 2000, **604**, 341–346.